

# Incorporating Platelet-Rich Plasma into Electrospun Scaffolds for Tissue Engineering Applications

Scott A. Sell, Ph.D.,<sup>1,2,\*</sup> Patricia S. Wolfe, B.S.,<sup>2,\*</sup> Jeffery J. Ericksen, M.D.,<sup>1,3</sup>  
 David G. Simpson, Ph.D.,<sup>4</sup> and Gary L. Bowlin, Ph.D.<sup>2</sup>

Platelet-rich plasma (PRP) therapy has seen a recent spike in clinical interest due to the potential that the highly concentrated platelet solutions hold for stimulating tissue repair and regeneration. The aim of this study was to incorporate PRP into a number of electrospun materials to determine how growth factors are eluted from the structures, and what effect the presence of these factors has on enhancing electrospun scaffold bioactivity. PRP underwent a freeze-thaw-freeze process to lyse platelets, followed by lyophilization to create a powdered preparation rich in growth factors (PRGF), which was subsequently added to the electrospinning process. Release of protein from scaffolds over time was quantified, along with the quantification of human macrophage and adipose-derived stem cell (ADSC) chemotaxis and proliferation. Protein assays demonstrated a sustained release of protein from PRGF-containing scaffolds at up to 35 days in culture. Scaffold bioactivity was enhanced as ADSCs demonstrated increased proliferation in the presence of PRGF, whereas macrophages demonstrated increased chemotaxis to PRGF. In conclusion, the work performed in this study demonstrated that the incorporation of PRGF into electrospun structures has a significant positive influence on the bioactivity of the scaffolds, and may prove beneficial in a number of tissue engineering applications.

## Introduction

**P**LATELET-RICH PLASMA (PRP) therapy is a method of collecting and concentrating autologous platelets, through centrifugation and isolation, for the purpose of activating and releasing their growth factor-rich  $\alpha$  and dense granules. The discharge of these concentrated granules releases a number of growth factors and cytokines in physiologically relevant ratios, although in concentrations several times higher than that of normal blood, that are critical to tissue regeneration and cellular recruitment. Some of the more highly concentrated factors found within PRP include platelet-derived growth factor (PDGF), transforming growth factor- $\beta$  (TGF- $\beta$ ), vascular endothelial growth factor (VEGF), fibroblast growth factor (FGF), and epidermal growth factor (EGF).<sup>1-7</sup> In addition, PRP has also been shown to contain a number of macrophage and monocyte mediators such as regulated upon activation, normal T-cell expressed, and secreted (RANTES), lipoxin, and an array of interleukins.<sup>1</sup>

Clinically, PRP therapy has been used to stimulate tissue growth and regeneration in a number of different tissues, effectively accelerating the healing response in patients suffering from osteochondral defects,<sup>2,7,8</sup> tendon/ligament in-

juries,<sup>2,6-11</sup> and chronic skin wounds (diabetic and pressure ulcers).<sup>3,7,8,12</sup> Typically, these procedures involve a blood draw and centrifugation to concentrate the platelet portion, followed by a platelet activation step and the delivery of the activated PRP to the site of injury. There have been several methods reported in the literature on successfully activating and delivering PRP to an injury site, with most involving the creation of a platelet gel using thrombin<sup>2,7,8,13</sup> or CaCl<sub>2</sub>.<sup>2,5,7,8</sup> These PRP gels can be easily applied to wound sites through injection or topical application.

However, studies have shown that the use of thrombin as a clotting agent can result in a rapid activation of platelets and a bolus release of growth factors, with 70% of growth factors released within 10 min of clotting, and nearly 100% released within 1 h.<sup>2</sup> This "dumping" method fails to maximize the cell stimulating potential of the PRP growth factors as most are cleared before they can take effect.<sup>14</sup> Growth factor release from PRP gels can be slowed when the gel is formed with CaCl<sub>2</sub> rather than thrombin. The addition of CaCl<sub>2</sub> to PRP results in the formation of autogenous thrombin from prothrombin and the eventual formation of a loose fibrin matrix that will secrete growth factors over 7 days.<sup>2</sup>

<sup>1</sup>Physical Medicine and Rehabilitation, Hunter Holmes McGuire VA Medical Center, Richmond, Virginia.

Departments of <sup>2</sup>Biomedical Engineering, <sup>3</sup>Physical Medicine and Rehabilitation, and <sup>4</sup>Anatomy and Neurobiology, Virginia Commonwealth University, Richmond, Virginia.

\*These authors contributed equally to this work.

Other techniques have been evaluated for further sustaining the release of growth factors from PRP and include the use of gelatin gel microspheres,<sup>15</sup> lyophilized PRP,<sup>16–19</sup> and alginate beads.<sup>14</sup> The injection of PRP gelatin gel microspheres in a mouse ischemic hind limb model demonstrated sustained release of the PRP potent angiogenic components as illustrated by an increase in perfusion, capillary density, and mature blood vessel density.<sup>15</sup> Alginate beads were shown to be successful in delivering (based on cell proliferation) PRP-derived growth factors and cytokines over the course of 14 days.<sup>14</sup> The use of freeze-dried PRP in a dermal wound has been shown to significantly increase cellular proliferation (up to 21 days), tissue regeneration, and angiogenesis in a mouse dermal wound.<sup>16–19</sup> Collectively, these studies demonstrate the importance of keeping PRP-derived growth factors and cytokines in the wound site and slowly releasing them as the wound site becomes infiltrated with reparative cells.

While a number of individual growth factors and/or cytokines have been used previously in an array of sustained release tissue engineering and regenerative medicine applications with positive results, the use of either single or multiple isolated growth factors/cytokines is often prohibitively expensive, and it can be difficult to replicate physiologically relevant quantities.<sup>2</sup> The aim of this study was to attempt to harness the reparative potential found in PRP, namely, the growth factor and cytokine milieu contained within, and apply it to tissue engineering through the creation of a PRP eluting electrospun scaffold. It was hypothesized that the inclusion of lysed and lyophilized PRP would create an effective preparation rich in growth factors (PRGF) capable of being introduced into the electrospinning process to create a scaffold with enhanced bioactivity capable of a sustained release of growth factors.

## Materials and Methods

### Creation of PRP and PRGF

Fresh human whole blood from three donors was purchased (Biological Specialty Corp.), pooled, and used in a SmartPREP<sup>®</sup> 2 (Harvest Technologies Corp.) centrifugation system to create PRP per manufacturers protocol. A small aliquot of both pooled whole blood and PRP were sent to the Harvard Immune Disease Institute's Blood Research laboratory to determine their respective platelet concentrations. PRP was then subjected to a freeze-thaw-freeze (FTF) cycle in a  $-70^{\circ}\text{C}$  freezer for cell lysis and activation. Centrifuge tubes containing PRP were placed in a  $-70^{\circ}\text{C}$  freezer for 24 h followed by a  $37^{\circ}\text{C}$  waterbath for 1 h, and then returned to the  $-70^{\circ}\text{C}$  freezer for 24 h. The degree of activation of the FTF lysed PRP, and thrombin (Recothrom; ZymoGenetics, Inc.) and 10%  $\text{CaCl}_2$  (American Regent)-activated PRPs was quantified through an enzyme-linked immunosorbent assay (ELISA) analysis of VEGF and basic fibroblast growth factor (bFGF) (Antigenix America Inc.). Frozen PRP was then lyophilized for 24 h to create a dry PRGF powder, which was finely ground in a mortar and pestle before use.

### Chemotactic effect of PRGF on macrophages

To determine the effect that powdered PRGF had on human macrophage chemotaxis, and to demonstrate that ly-

ophilized PRGF retained viable chemotactic proteins, PRGF was dissolved in macrophage serum-free medium (MSFM; Invitrogen) in a range of concentrations (0, 0.01, 0.1, 1, 5, and 10 mg/mL). Using a 24-well Transwell plate with 8- $\mu\text{m}$ -diameter pores (Corning, Inc.), 600  $\mu\text{L}$  of PRGF-containing medium was placed in the bottom wells, whereas the top insert was seeded with 100,000 human peripheral blood macrophages (ATCC, CRL9855) in 150  $\mu\text{L}$  of control medium for 18 h ( $n=3$ ). After 18 h, the bottom wells were aspirated and the average cell number was determined through the use of an automated cell counter (Invitrogen Countess).

### Creation of PRGF eluting electrospun scaffolds

Scaffolds used in this study consisted of silk fibroin (SF, extracted from *Bombyx morii* silkworm cocoons<sup>20,21</sup>), poly (glycolic acid) (PGA; Alkermes), and polycaprolactone (PCL; Lakeshore Biomaterials, 125 kDa). Each of these materials was dissolved in 1,1,1,3,3,3 hexafluoro-2-propanol (HFP; TCI America, Inc.) at a concentration of 100 mg/mL to create the solutions used in the electrospinning process. These materials were chosen as they are three commonly used biomaterials that have been well characterized, and have well-known degradation characteristics.

To each of these electrospinning solutions, PRGF was added in concentrations of 10 or 100 mg of PRGF per milliliter of electrospinning solution (SF:PRGF(10), PGA:PRGF(10), and PCL:PRGF(10) and SF:PRGF(100), PGA:PRGF(100), and PCL:PRGF(100), respectively) and allowed to dissolve completely into solution. As PRGF can be successfully electrospun by itself from HFP at a concentration of 200 mg/mL<sup>22</sup>, PRGF fibers were also integrated into PCL scaffolds using two additional electrospinning techniques: (1) a 2 input-1 output nozzle that mixed separate PCL and PRGF solutions only at the outlet tip as electrospinning occurred (PCL:PRGF(2–1)) and (2) using two separate syringes of PCL and PRGF electrospinning solutions at  $90^{\circ}$  from each other targeting the same collection mandrel (PCL:PRGF). Both the PCL:PRGF(2–1) and PCL:PRGF scaffolds consisted of a 1:1 volume ratio of PCL:PRGF solution. Control scaffolds contained no PRGF.

Processing parameters varied with the polymer, whereas all solutions were electrospun onto a grounded rectangular stainless steel mandrel (1.9 cm wide  $\times$  7.5 cm long  $\times$  0.5 cm thick) rotating at 400 RPM and translating at 6 cm/s over a distance of 12 cm, using a Becton Dickinson syringe fitted with a blunt tip 18 gauge needle and a KD Scientific syringe pump. SF solutions were electrospun using a charging voltage of +25 kV, an air gap distance of 15 cm, and a flow rate of 4 mL/h. PGA and PCL solutions were electrospun using a charging voltage of +22 kV, an air gap distance of 15 cm, and a flow rate of 6 mL/h. PCL:PRGF(2–1) used a charging voltage of +30 kV placed on the end of the output nozzle, an air gap distance of 15 cm, and a flow rate of 2.5 mL/h. PCL:PRGF used charging voltages of +25 and +27 kV for the PCL and PRGF solutions, respectively, an air gap distance of 15 cm from each syringe to the collecting mandrel, and a flow rate of 2.5 mL/h for each solution.

### Characterization of electrospun structures

Dry, representative samples from each of the electrospun scaffolds were characterized through scanning electron microscopy (SEM; Zeiss EV050) to ensure the fibrous nature of

the structures. Average fiber diameters and pore areas were calculated by taking 60 random fiber/pore measurements from across the SEM image using ImageTool 3.0 software (Shareware provided by UTHSCSA).

Uniaxial tensile testing was performed on a set of representative dog-bone-shaped samples (overall length of 20 mm, 2.67 mm at its narrowest point, gage length of 7.5 mm,  $n=5$ ) punched from each of the materials electrospun. All specimens were soaked for 4 h in deionized water before testing, with all SF samples first being soaked in ethanol for 30 min to promote beta sheet formation. Samples were then uniaxially tested to failure at a rate of 10 mm/min ( $1.33 \text{ min}^{-1}$  strain rate) using an MTS Bionix 200 testing system with a 100 N load cell (MTS Systems Corp.). Peak stress, modulus, and strain at break were calculated using TestWorks version 4.

#### Evaluation of cell interaction

To determine the response of human cells on the PRGF-containing scaffolds, 10-mm-diameter disks from each electrospun scaffold were punched, disinfected (30 min soak in ethanol followed by three 10 min rinses in phosphate-buffered saline [PBS]), and placed in a 48-well plate. Each scaffold had a sterile Pyrex cloning ring (10 mm outer diameter, 8 mm inner diameter) placed on top to keep the scaffolds from floating, and to ensure that all cells stayed on the surface of the scaffold during culture. Each scaffold was then seeded with 50,000 human adipose-derived stem cells (ADSC) in 500  $\mu\text{L}$  of culture medium (Dulbecco's modified Eagle's medium low glucose, 10% fetal bovine serum, 1% penicillin/streptomycin; Invitrogen). Medium was changed every third day, and samples were removed from culture and fixed in buffered formalin on days 7 and 21 for hematoxylin and eosin (H&E) staining.

#### Quantification of protein release kinetics

From each electrospun material 10-mm-diameter disks were punched ( $n=3$ ), disinfected (30 min soak in ethanol followed by three 10 min rinses in PBS), and placed in a 48-well plate with 500  $\mu\text{L}$  of PBS. The PBS was changed and retained for evaluation on days 1, 4, 7, 10, 14, 21, 28, and 35. Samples at each time point were subjected to a generic protein assay (BCA Protein Assay; Thermo Scientific Pierce) to quantify the concentration of total protein released. Based upon these results, specific ELISAs were run on the retained samples (days 1, 4, 7, 10, 14, and 21) to detect proteins found in high concentrations in PRP, RANTES, PDGF-BB (Antigenix America, Inc.), and TGF- $\beta$  (Promega Corp.), to demonstrate that it was in fact PRGF being eluted from the scaffolds.

#### Released PRGF effect on cell proliferation

To determine the mitogenic potential of the PRGF released from the electrospun scaffolds on both ADSCs and macrophages, 10-mm-diameter disks of each electrospun material were punched, disinfected (30 min soak in ethanol followed by three 10 min rinses in PBS), and placed in a 48-well plate ( $n=3$ ). Each well was then seeded with 300,000 human peripheral blood macrophages (ATCC, CRL9855) in 500  $\mu\text{L}$  MSFM, as well as in a control tissue culture polystyrene (TCPS) well containing MSFM with 1 mg/mL PRGF added

(TCPS:PRGF). The macrophage-conditioned medium was removed daily and used as a supplement to feed ADSCs (200  $\mu\text{L}$  MSFM with 300  $\mu\text{L}$  ADSC medium) cultured on TCPS (25,000 cells/well) in a separate 48-well plate. On days 1, 4, and 7, the medium was removed from the wells containing macrophages and replaced with 300  $\mu\text{L}$  trypsin to remove macrophages for counting. After 5 min trypsin was deactivated with 300  $\mu\text{L}$  MSFM, pipetted up and down gently several times, and the suspended macrophages were counted using an automated cell counter (Invitrogen Countess). ADSC proliferation was analyzed using an MTS Assay (Promega) at days 1, 4, and 7.

This study was then replicated without the use of macrophage-conditioned medium to isolate the impact of the released PRGF on ADSC proliferation. That is, disinfected 10-mm-diameter disks of each electrospun material were placed in a 48-well plate with 500  $\mu\text{L}$  ADSC culture medium. The medium was removed daily and used as a supplement to feed ADSCs cultured at 25,000 cells/well in a separate 48-well plate. ADSC proliferation was determined with an MTS Assay (Promega) at days 1, 4, and 7.

#### Statistical analysis

All statistical analysis was based on a Kruskal–Wallis one-way analysis of variance on ranks and a Tukey–Kramer pairwise multiple comparison procedure ( $\alpha=0.05$ ) performed with the JMP<sup>®</sup> IN 8.0 statistical software package (SAS Institute, Inc.). Graphical depictions of mean data were constructed with Microsoft Excel 2007, with error bars representing standard deviations.

## Results

#### Creation of PRP and PRGF

Based upon the platelet counts performed at the Harvard Immune Disease Institute's Blood Research laboratory, it was determined that the pooled whole blood used for this study contained  $175 \times 10^3$  platelets/ $\mu\text{L}$ , whereas the PRP created with the SmarPreP<sup>2</sup> system yielded  $955 \times 10^3$  platelets/ $\mu\text{L}$ .

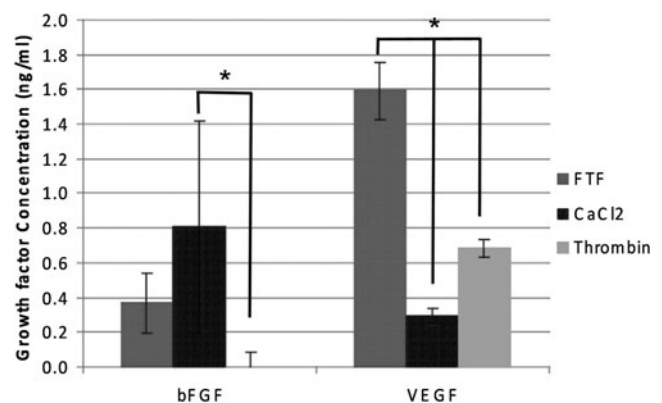


**FIG. 1.** Results of platelet-rich plasma activation method on bFGF and VEGF concentration. \*Significant differences between activation methods,  $p < 0.05$ . Minimum levels of detection for bFGF and VEGF were 0.11 ng/mL and 0.059 ng/mL, respectively. bFGF, basic fibroblast growth factor; VEGF, vascular endothelial growth factor; FTF, freeze-thaw-freeze.

This 5.5-fold increase in platelets is consistent with published data,<sup>23</sup> and should result in a similar fold increase in growth factor concentration based upon the linear relationship between platelet and growth factor concentration.<sup>24</sup>

The results of the bFGF and VEGF ELISAs (Fig. 1) reveal the FTF method of activation, essentially lysing platelets to release their  $\alpha$  and dense granule contents, to be as effective, if not more so, than the traditional PRP activation techniques of thrombin and  $\text{CaCl}_2$  for releasing growth factors. The FTF activation method resulted in average growth factor concentrations of 0.4 ng/mL for bFGF, and 1.6 ng/mL for VEGF. Using the traditional  $\text{CaCl}_2$  and thrombin activation methods, bFGF values were 0.8 and 0 ng/mL, respectively, whereas the VEGF values were 0.3 and 0.7 ng/mL, respectively. While there were few statistical differences between the different methods in the bFGF ELISA, with only the  $\text{CaCl}_2$  activated different from the thrombin activated, the VEGF ELISA results demonstrated clearly that the FTF method was significantly greater than the other activation methods. It should be noted that the thrombin activation method resulted in an instantaneous gel, making it difficult to obtain liquid samples for ELISA analysis. The  $\text{CaCl}_2$ -activated PRP contained visible floating platelet aggregates, but was mostly liquidous, whereas the FTF-activated PRP was completely liquid with no evidence of platelet aggregation.

#### Chemotactic effect of PRGF on macrophages

The results of macrophage chemotaxis in response to a dose of PRGF dissolved in MSFM are shown in Figure 2. Macrophage chemotaxis increased with the amount of PRGF until the concentration of 1 mg/mL, above which it became significantly reduced. While a nice trend is apparent, the only value that was significantly different from the group was the 1 mg/mL PRGF concentration, potentially indicating an ideal concentration for stimulating macrophage chemotaxis. It should be noted that the addition of powdered PRGF to MSFM resulted in a complete gel at 10 mg/mL, and a partial gel at 5 mg/mL. This resulting gelation may have had a negative impact on macrophage chemotaxis; however, it does indicate a reserve of active fibrinogen contained within

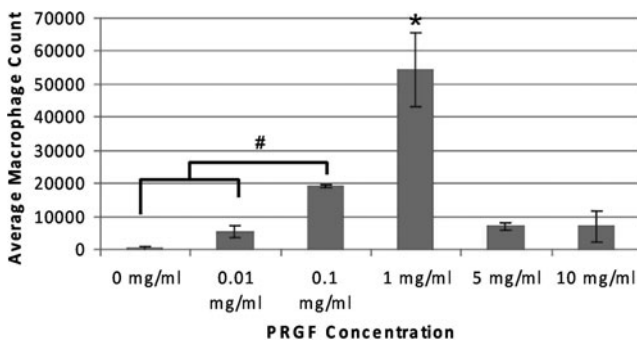


FIG. 2. Results of macrophage chemotaxis in response to PRGF dose. \*Statistically significant differences,  $p < 0.05$ , between the 1 mg/mL concentration and all other groups. #Statistically significant differences,  $p < 0.05$ , between 0.1 mg/mL and lower concentrations. PRGF, preparation rich in growth factors.

the powdered PRGF capable of forming a clot in the presence of the  $\text{Ca}^{2+}$  found in the MSFM.

#### Characterization of electrospun structures

The results of the electrospun scaffold SEM characterization are shown in Figure 3. These SEMs demonstrate the fibrous nature of each of the electrospun scaffolds, both with and without PRGF. Mean fiber diameters for these scaffolds ranged from 0.5  $\mu\text{m}$  for PGA:PRGF(10) to 5.8  $\mu\text{m}$  for SF:PRGF(100). With the exception of the SF:PRGF(100), there were no significant differences in mean fiber diameter between the control scaffolds and the PRGF-containing scaffolds. Somewhat surprisingly, the inclusion of PRGF had no real impact on the average size of the electrospun fibers, although it does appear that with the inclusion of high concentrations of PRGF and in the PCL:PRGF(2-1) and PCL:PRGF scaffolds there are a number of extremely small-diameter fibers. Disregarding the SF scaffolds, this potential divergent population of PRGF fibers and synthetic polymer fibers may be evident through the rather large standards of deviation determined for those structures. Additionally, those same scaffolds appeared to exhibit an increase in void space visible in the SEMs as PRGF content was increased. Average pore areas (Fig. 3) were found to correlate to average fiber diameters: as fiber diameter increased, pore area increased. This phenomenon has been well documented in previous electrospinning studies.<sup>25-27</sup>

The addition of 100 mg/mL PRGF to SF and PGA resulted in significantly increased pore areas over the control and 10 mg/mL PRGF-containing samples, whereas the only difference seen in the PCL structures was between the PCL:PRGF(2-1) and the PCL:PRGF(100), PCL:PRGF(10), and PCL control scaffolds.

The results of the scaffold uniaxial tensile testing are shown in Figure 4. Mean peak stresses ranged from 0.2 MPa for PGA:PRGF(100) to 5.2 MPa for PGA control, moduli ranged from 0.9 MPa for SF+100 to 21.4 MPa for PGA control, whereas average strain at break values ranged from 25.4% for PGA:PRGF(100) to 112.8% for PGA control. In general, mechanical properties were shown to decrease significantly as PRGF concentration increased compared to values achieved for the PRGF-free control scaffolds. With the exception of the PCL:PRGF(10), average peak stresses and moduli were significantly lower for SF, PGA, and PCL scaffolds containing PRGF. These results were not unexpected, as traditionally the combination of biologic proteins in large concentrations (collagen, elastin, fibrinogen, etc.) with electrospun polymers regarded for their tensile strength typically results in significantly reduced mechanical strength.<sup>28-30</sup>

The unique structures of PCL:PRGF(2-1) and PCL:PRGF, where both PRGF and PCL fibers were created, resulted in mechanical properties that fell between those of the PCL control and the PCL:PRGF(100) structures. This difference in mechanical properties would seem to indicate that these blended scaffolds resulted in materials that were structurally different from those where PRGF was added directly to the electrospinning solution. Additional work will be needed to fully differentiate the differences between the two methods of PRGF inclusion, and to understand what role individual PRGF fibers may play in providing/reducing mechanical strength of the scaffolds.

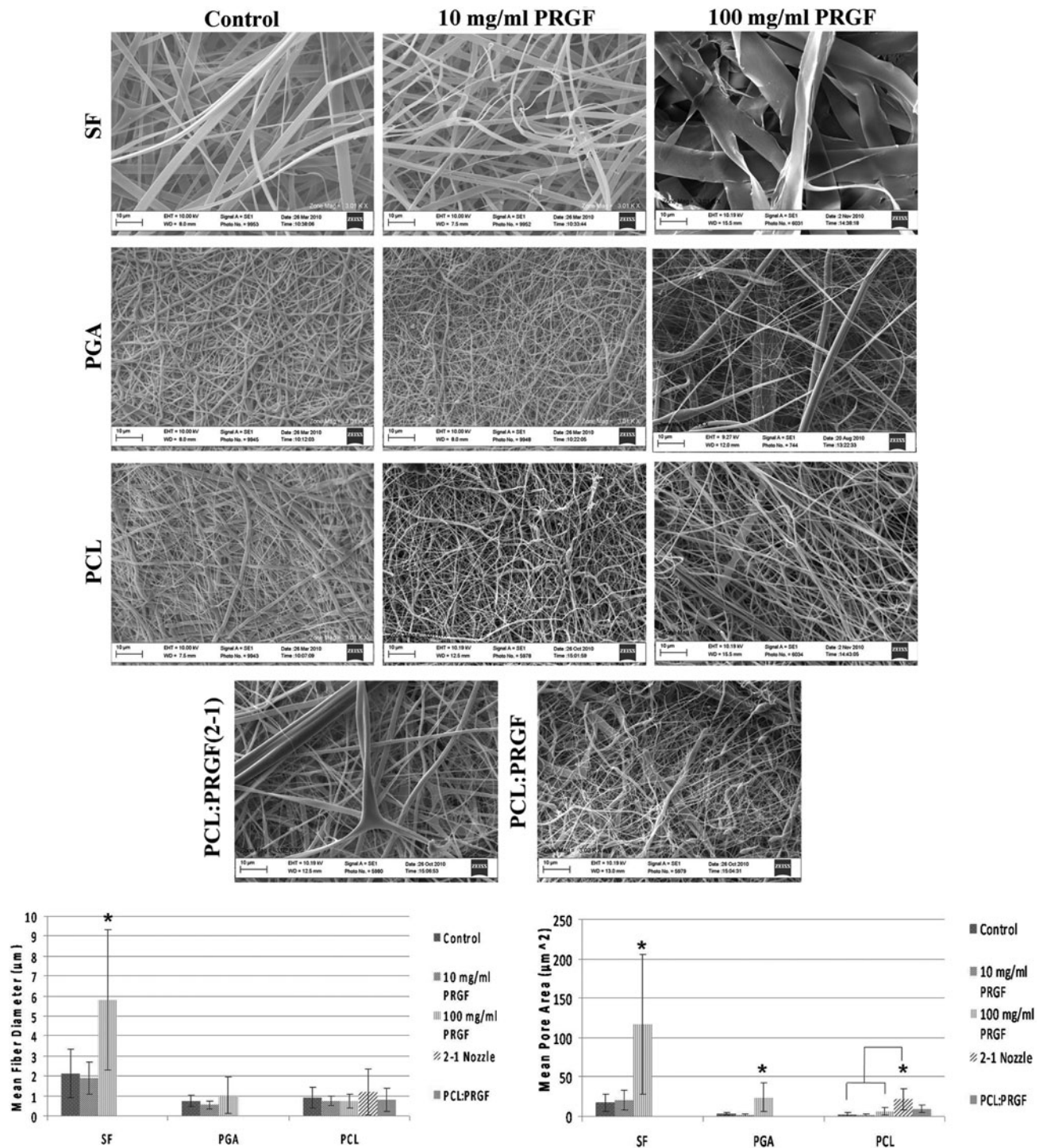
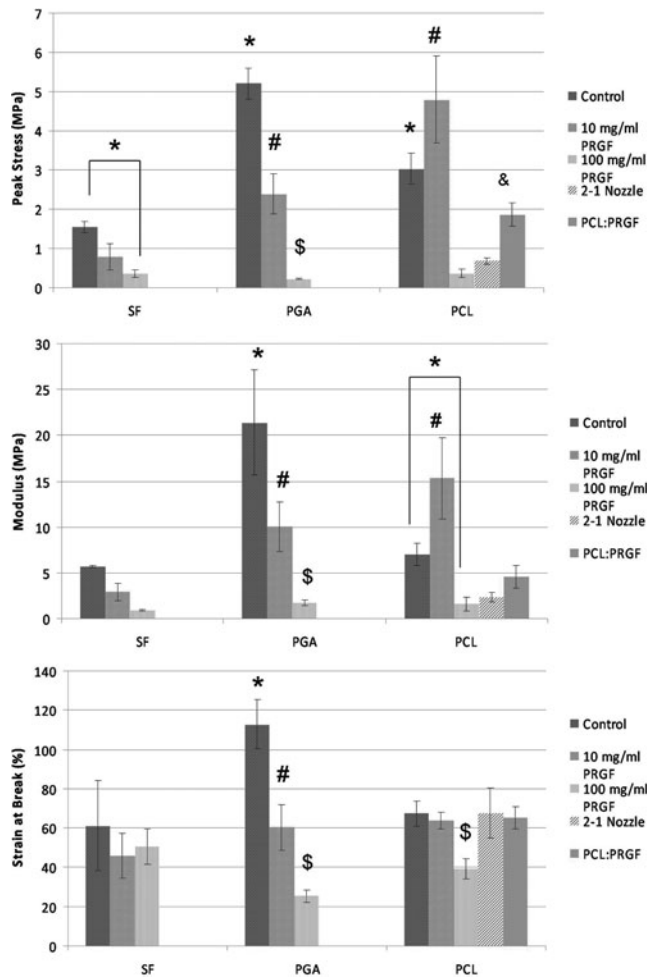


FIG. 3. (Top) SEM micrographs of electrospun SF, PGA, and PCL scaffolds with and without PRGF. All images were taken at 3000×; scale bar is 10 μm. (Bottom left) Graph of mean fiber diameters for SF, PGA, and PCL scaffolds with and without PRGF. (Bottom right) Graph of mean pore areas for SF, PGA, and PCL scaffolds with and without PRGF. \*Significant differences within polymer group,  $p < 0.05$ . SF, silk fibroin; PGA, poly(glycolic acid); PCL, polycaprolactone.

Evaluation of cell interaction

The results of the H&E staining are shown in Figures 5 and 6. H&E staining revealed confluent layers of ADSCs on the surfaces of the control scaffolds by day 7, whereas increased PRGF content resulted in increased cellular pene-

tration into the scaffold. Surprisingly, after only 7 days ADSCs had migrated through half of the thickness of the PCL:PRGF(2-1) scaffold. By day 21 this trend was even more apparent, with clear cell migration through nearly the entire thickness of the PCL:PRGF(2-1) and PCL:PRGF scaffold (Fig. 7). The SF:PRGF(100) scaffold also had nearly complete



**FIG. 4.** Results of uniaxial tensile testing of electrospun scaffolds. \*Statistically significant differences,  $p < 0.05$ , between control scaffolds and scaffolds containing PRGF. #Statistically significant differences,  $p < 0.05$ , between scaffolds containing 10 mg/mL PRGF and other scaffolds. \$Statistically significant differences,  $p < 0.05$ , between scaffolds containing 100 mg/mL PRGF other scaffolds. &Statistically significant differences,  $p < 0.05$ , between PCL:PRGF scaffolds and other scaffolds.

cellular penetration by day 21, compared to the SF scaffold containing no PRGF, which exhibited only minimal migration into the depth of the structure. The PCL:PRGF(100) demonstrated a similar result, with the electrospun synthetic PCL material traditionally being difficult to cellularize *in vitro*,<sup>20,31,32</sup> as it too exhibited increased cellular penetration when compared to the PCL scaffold containing no PRGF.

#### Quantification of protein release kinetics

The results of quantified protein release from PRGF-containing scaffolds are shown in Figure 8. The results of this study demonstrated that scaffolds containing high concentrations of PRGF (SF:PRGF(100), PGA:PRGF(100), PCL:PRGF(100), and PCL:PRGF(2-1)) released detectable amounts of protein over 35 days in culture. The protein release from PRGF-containing scaffolds peaked at day 1, de-

creased by about half on days 4 and 7, and reached a plateau that was sustained for the remainder of the duration. PCL:PRGF(2-1) scaffolds initially had the highest release of protein (300  $\mu\text{g/mL}$ ), but PCL:PRGF(100) had the highest release of protein at all time points after day 1 (125–50  $\mu\text{g/mL}$ ). Surprisingly, PCL:PRGF scaffolds released the lowest amount of protein over the 35 days, even though the concentration of PRGF incorporated was the same as that of PCL:PRGF(2-1) scaffolds. PGA:PRGF(100) and SF:PRGF(100) scaffolds had similar release kinetics as well, eliciting 240 and 275  $\mu\text{g/mL}$  of protein at day 1, respectively. Similar to the PCL:PRGF(100) and PCL:PRGF(2-1) structures, a plateau was achieved around 50  $\mu\text{g/mL}$  and sustained until day 35. Minimal protein release was detected for PGA, SF, and PCL control scaffolds and scaffolds containing 10 mg/mL PRGF over the 35 days, indicating that the protein detected was in fact due to PRGF release and not simply an artifact of scaffold degradation.

Statistical analysis revealed protein release at day 1 from scaffolds of PGA:PRGF(100), SF:PRGF(100), PCL:PRGF(100), and PCL:PRGF(2-1) to be significantly greater than protein release from those respective scaffolds at all other time points (day 4–35). Additionally, scaffolds of PCL:PRGF(100) had significantly greater release at day 4 than at day 35. The initial burst of release from the scaffolds at day 1 was expected as PRGF from the surface of the scaffolds was released. Remarkably, after the first day there was still a sustained release of protein from scaffolds of PGA:PRGF(100), SF:PRGF(100), PCL:PRGF(100), and PCL:PRGF(2-1) that continued throughout the 35 days, presumably due to the degradation of the polymer scaffolds and subsequent release of entrapped proteins.

Quantification of RANTES, PDGF-BB, and TGF- $\beta$  from the PRGF-containing scaffolds revealed detectable release over 21 days (Fig. 9) with kinetics similar to those of the protein assay results described previously. Scaffolds of PCL:PRGF(100) had the highest release of RANTES at day 1 (3 ng/mL), with a continual decrease in release thereafter. PGA:PRGF(100), SF:PRGF(100), and PCL:PRGF(2-1) exhibited a similar trend, with peak values of RANTES at day 1 of 2.5 ng/mL, 1.1 ng/mL, and 1 ng/mL for each scaffold, respectively. RANTES release from PCL:PRGF scaffolds had a peak of 0.5 ng/mL at day 1, but values were not detectable after day 4. Statistical analysis revealed that RANTES release at day 1 from scaffolds of PGA:PRGF(100), SF:PRGF(100), PCL:PRGF(100), and PCL:PRGF(2-1) was significantly higher than that from those same scaffolds at all other time points (days 4–21). For PCL:PRGF(100), RANTES release at day 4 was significantly higher than that of all other time points for that scaffold.

PDGF-BB release was highest from scaffolds of PCL:PRGF(2-1), peaking at day 1 (0.3 ng/mL), and decreasing thereafter, with values not detectable after day 7. PDGF-BB was also detectable from scaffolds of PGA:PRGF(100), SF:PRGF(100), and PCL:PRGF(100), with the highest release occurring at day 1 (0.1 ng/mL, 0.075 ng/mL, and 0.15 ng/mL, respectively). PCL:PRGF scaffolds elicited PDGF-BB release of 0.03 ng/mL at day 1, but was undetectable thereafter. PDGF-BB release at day 1 from scaffolds of PGA:PRGF(100), PCL:PRGF(100), and PCL:PRGF(2-1) was significantly higher than release from those same scaffolds at all other time points (days 4–21).

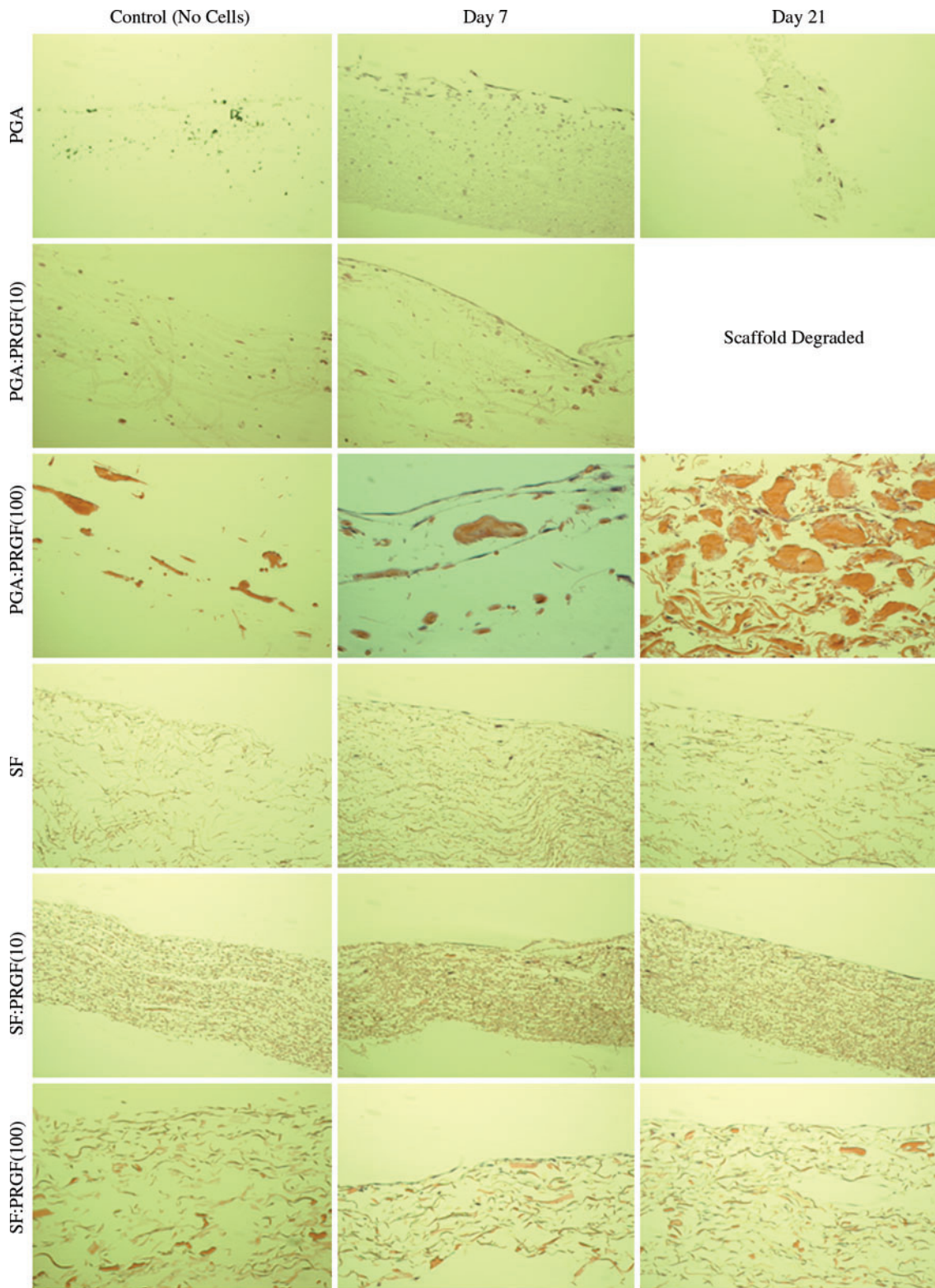


**FIG. 5.** H&E staining of PGA and SF scaffolds at days 7 and 21. Images at 20 $\times$ . Note, the PGA:PRGF(10) scaffold was completely degraded by day 21 and was unable to be processed for histological evaluation. H&E, hematoxylin and eosin. Color images available online at [www.liebertonline.com/tea](http://www.liebertonline.com/tea)

PDGF-BB release from SF:PRGF(100) at day 1 was significantly greater than release from the same scaffold at days 7–21. For PCL:PRGF(100) and PCL:PRGF(2-1), PDGF-BB release at day 4 was significantly higher than that of days 10–

21 and all other time points with detectable values, respectively, for those scaffolds.

Much like the release of PDGF-BB from the scaffolds, TGF- $\beta$  release was highest from scaffolds of PCL:PRGF(2-1). Peak

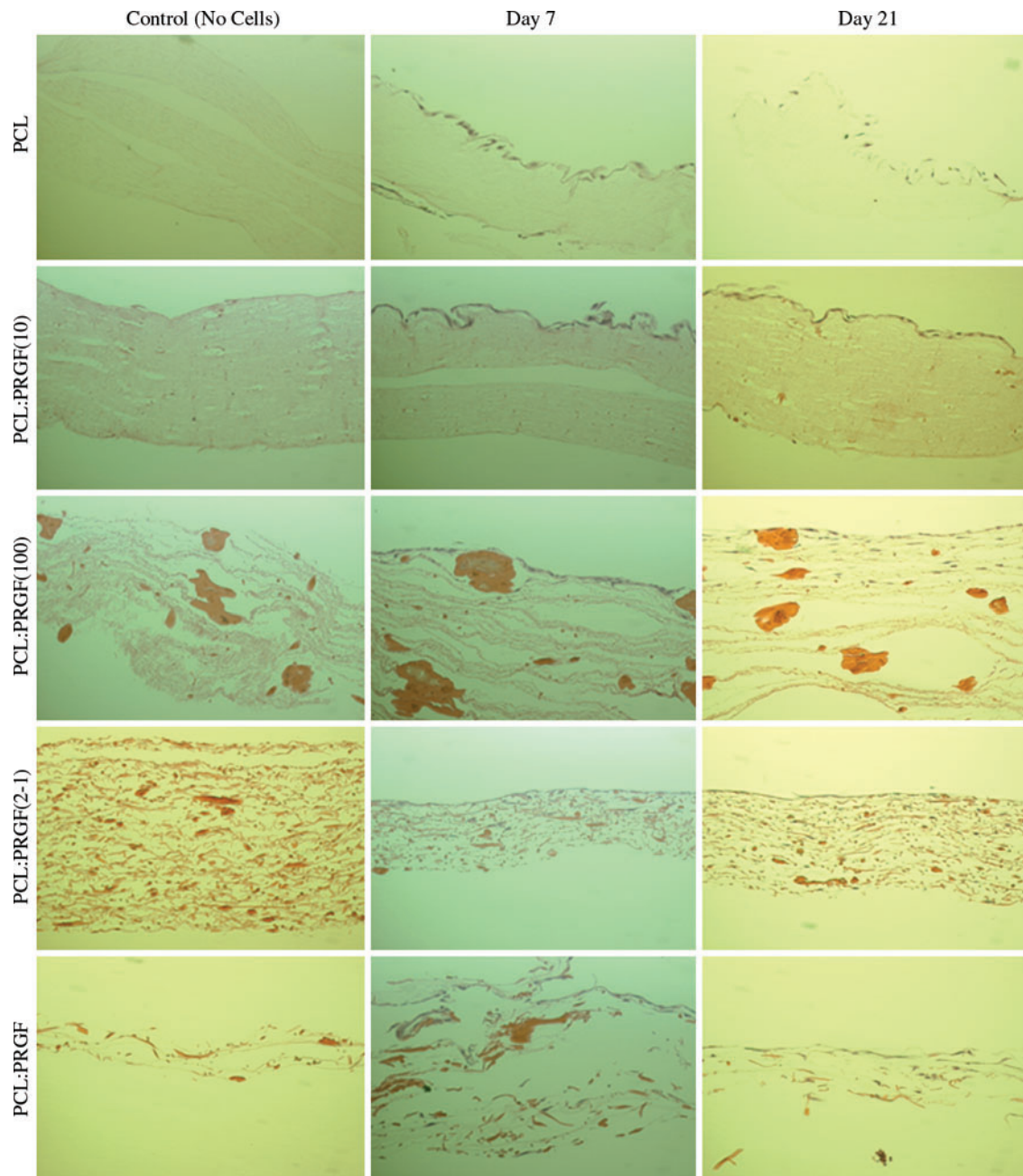


**FIG. 6.** H&E staining of PCL scaffolds at day 7 and 21. Images at 20 $\times$ . Color images available online at [www.liebertonline.com/tea](http://www.liebertonline.com/tea)

release was seen on day 4 (1.17 ng/mL), although not significantly different from the release on day 1 (1.13 ng/mL), and decreased thereafter. Unlike RANTES and PDGF-BB, TGF- $\beta$  release values were quantifiable for the PCL:PRGF(2-1), PCL:PRGF(100), and SF:PRGF(100) scaffolds throughout the 21 days evaluated. TGF- $\beta$  release from scaffolds of PCL:PRGF(100) and PCL:PRGF(2-1) was significantly higher at days 1 and 4 than release from those same scaffolds at all other time points (days 7–21). In addition, release of TGF- $\beta$  from scaffolds of PCL:PRGF(2-1) at days 7 and 10 was significantly higher than that at days 14 and 21. Surprisingly, PGA:PRGF(100) scaffolds did not exhibit a release above the minimum level of detection over the 21 days.

Similar to the protein assay results, RANTES, PDGF-BB, and TGF- $\beta$  were undetectable from both the PGA, SF, and PCL control scaffolds and the scaffolds containing 10 mg/mL PRGF at all time points. The results of the statistical analysis illustrated that, in general, after the initial release of growth factors from the surface of the scaffold at day 1, the release of RANTES and PDGF-BB that occurred at all time points thereafter is not significantly different, demonstrating a sustained release of growth factors from the scaffolds over the 21-day period as the polymer fibers begin to degrade. With regard to TGF- $\beta$ , the PCL:PRGF(2-1) scaffolds exhibited a step-wise significant decrease in release until day 14, but still maintained a sustained quantifiable release.

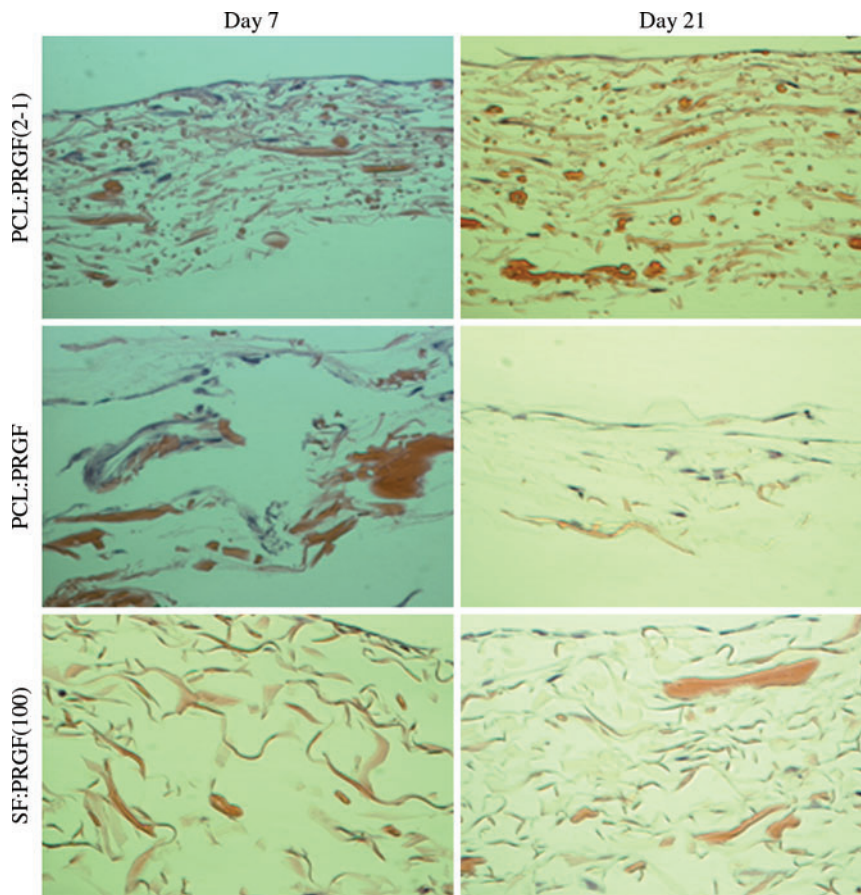


**FIG. 7.** High-magnification (40 $\times$ ) images of select scaffolds demonstrating significant cellular penetration. Color images available online at [www.liebertonline.com/tea](http://www.liebertonline.com/tea)

#### Released PRGF effect on cell proliferation

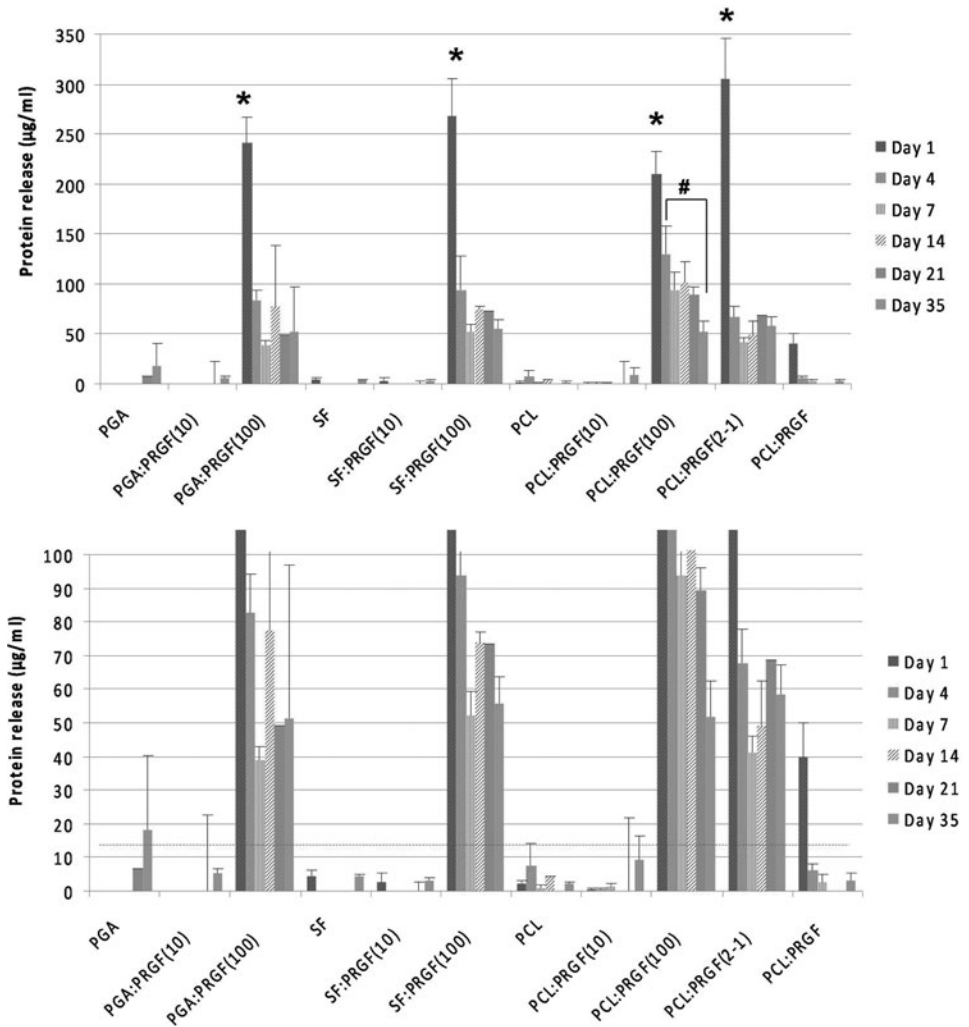
The effect of PRGF release on macrophage proliferation is shown in Figure 10. As expected, macrophages proliferated in the presence of all scaffolds from days 1 and 4; however, by day 7 proliferation slowed, and in some cases, cell number even decreased. This may be due to nutrient levels insufficient to support the large number of cells in each well, and hence, resultant cell apoptosis. At day 1, there was no significant difference in macrophage number between the different scaffolds and TCPS. At day 4, there were significantly less macrophages on scaffolds of PCL:PRGF(2-1) than on scaffolds of SF, SF:PRGF(10), TCPS, and TCPS:PRGF, and may indicate a loss of macrophages due to cellular penetration into the highly bioactive PCL:PRGF(2-1) scaffolds. By day 7, there were no significant differences in macrophage proliferation on any scaffold. While these results indicated that, in general, PRGF did not have an effect on macrophage proliferation, taken with the results from the prior macrophage chemotaxis study, it could instead be anticipated that PRGF promotes macrophage chemotaxis rather than proliferation.

To determine the role that PRGF had in the secretion of macrophage growth factors, ADSCs were cultured in medium conditioned by macrophages exposed to released PRGF. The results of ADSC proliferation, when cultured in macrophage-conditioned medium, demonstrated no significant differences in proliferation at day 1. However, by day 4 ADSCs cultured in macrophage-conditioned medium from scaffolds of PCL:PRGF(100) and PCL:PRGF(2-1) had significantly greater

proliferation than ADSCs cultured in macrophage-conditioned medium from the PCL and TCPS control, as well as all other scaffolds (Fig. 11). By day 7, there was significantly greater ADSC proliferation in macrophage-conditioned medium from scaffolds of PCL:PRGF(100), PCL:PRGF(2-1), and TCPS:PRGF than ADSCs cultured in conditioned medium from PCL and TCPS control, as well as all other scaffolds. This was expected, as it had previously been demonstrated that PRGF, as well as growth factors secreted by macrophages, enhanced fibroblast, mesenchymal, and stromal stem cell proliferation.<sup>2,33–37</sup> In general, ADSC proliferation in all pre-conditioned medium increased from day 1 to day 4; however, by day 7 it appeared that proliferation slowed, and in some cases cell number even decreased, potentially due to induced contact inhibition as the cells became confluent in the wells, or died off following exhaustion of medium nutrients. This may also have been because the conditioned medium used for the ADSCs was MSFM, which is unfavorable over the long-term for ADSC growth, or due to harmful factors expressed during macrophage apoptosis.<sup>38</sup> From the results in Figure 10, it was evident that the effect of macrophages on ADSC proliferation was due to macrophage interaction with PRGF-containing scaffolds, and not the number of macrophages.

ADSC proliferation when cultured in PRGF-conditioned medium without macrophages is displayed in Figure 12. Overall, ADSCs proliferated from day 1 to day 4 (with a few exceptions), and from day 4 to day 7, as expected. After 1 day, there were no significant differences in ADSC proliferation for any scaffold. By day 4, ADSCs cultured in

**FIG. 8.** Quantification of generic protein released from PRGF-containing scaffolds over 35 days (Top). \*Significant difference,  $p < 0.05$ , for day 1 when compared to all other time points for each material. #Statistically significant differences,  $p < 0.05$ , between day 4 and day 35 of PCL:PRGF(100). Y-axis scaled to emphasize decreased release from days 4 to 35 (bottom). Minimum level of detection was 14.3  $\mu\text{g}/\text{mL}$  (dashed line).



medium from scaffolds of SF:PRGF(100) had significantly greater proliferation than those cultured in medium from SF control scaffolds. At day 7, ADSCs cultured in medium from scaffolds of SF:PRGF(100) and PCL:PRGF(2-1) had significantly greater proliferation than cells cultured in medium from SF and PCL control scaffolds, respectively. Compared to ADSCs cultured in medium from the TCPS control, cells cultured in medium from PCL:PRGF(2-1) and PCL:PRGF scaffolds had significantly greater proliferation at day 7. These results suggest that the presence of PRGF does impact ADSC proliferation, and corroborates previously published work.<sup>2,33-35,37</sup> It is clearly evident from these studies that the proliferation of ADSCs, cultured in conditioned medium, is different depending on the presence or absence of macrophages and macrophage-secreted factors over the 7-day study duration, and will be discussed further in the following section.

**Discussion**

This present study provides a proof of principle for the incorporation of a powdered PRGF derived from human PRP into electrospun scaffolds of a number of materials. Through a number of evaluation methods, we were able to demonstrate that PRGF retained its physiologic activity after

lyophilization and through the electrospinning process, subsequently enhancing the bioactivity of the electrospun scaffolds.

The use of PRP in clinical applications has been gaining in popularity as a means to stimulate tissue repair and regeneration with very minimal risk to the patient. However, the “black box” approach taken by many of the clinicians utilizing PRP leaves much to be done in the realm of basic science to fully understand and standardize the practice. To date, the collection of whole blood and the concentration and isolation of platelets to make PRP has been proven effective *in vitro* for stimulating cellular activity in a number of formats, both in liquid<sup>13,33-35,37,39-41</sup> and in lyophilized PRGF form.<sup>16-19</sup>

To the best of the authors’ knowledge, this article serves as the first instance of a powdered PRGF being incorporated into an electrospun tissue engineering scaffold to serve as a controlled release vehicle for such a concentrated growth factor and cytokine milieu. While electrospun scaffolds have been used as growth factor delivery systems in the past,<sup>42-47</sup> they have typically been limited to the incorporation of only a small number of growth factors due in part to the cost associated with purchasing the recombinant or isolated proteins.<sup>44</sup> The incorporation of a cost-effective PRGF protein array into an electrospun structure has the

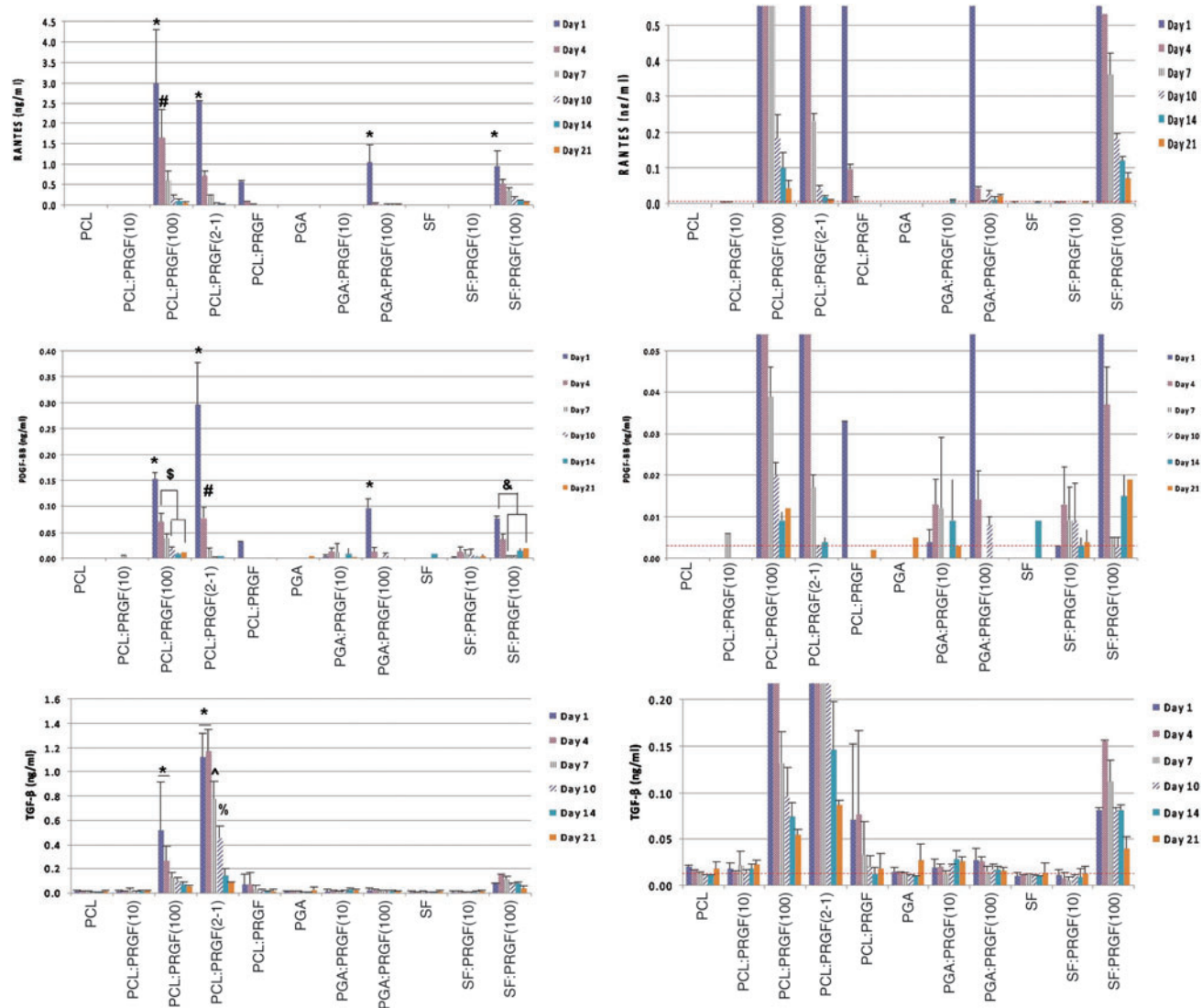


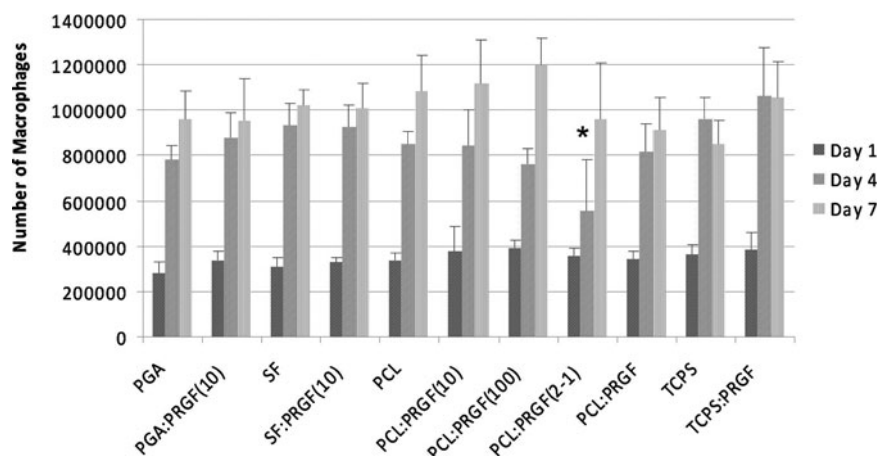
**FIG. 9.** Results of RANTES, PDGF-BB, and TGF- $\beta$  release from PRGF-containing scaffolds 21 days. \*Statistically significant differences,  $p < 0.05$ , between day 1 and all other time points. #Statistically significant differences,  $p < 0.05$ , between day 4 and all other time points. %Statistically significant differences,  $p < 0.05$ , between day 4 and days 10 and 21. ^Statistically significant differences,  $p < 0.05$ , between day 7 and all other time points. %Statistical significance,  $p < 0.05$ , between day 10 and all other time points. Minimum levels of detection for RANTES, PDGF-BB, and TGF- $\beta$  were 0.001 ng/mL, 0.003 ng/mL, and 0.011 ng/mL, respectively (dashed line). RANTES, regulated upon activation, normal T-cell expressed, and secreted; PDGF, platelet-derived growth factor; TGF- $\beta$ , transforming growth factor- $\beta$ . Color images available online at [www.liebertonline.com/tea](http://www.liebertonline.com/tea)

potential to deliver a multitude of growth factors, cytokines, and chemokines in physiologically relevant ratios. Such a platelet-based growth factor cocktail would essentially replicate the necessary factors found in a site of normal wound healing and promote the formation of healthy tissue through the stimulation of the healing cascade.<sup>48</sup> The results presented in this article demonstrated the potential of such a sustained release vehicle through enhanced cellular activity consistent with other *in vitro* studies of PRP/PRGF.

Cellular migration and penetration into electrospun scaffolds was enhanced, regardless of polymer, with the addition of PRGF. While historically the ability for cells to migrate into an electrospun structure has been viewed as a challenge, especially with synthetic polymers such as PGA and

PCL,<sup>20,31,32</sup> the inclusion of PRGF yielded structures that were readily infiltrated. The reason for this rapid infiltration is not yet fully understood in this preliminary investigation, and will need further investigation. However, the presence of an array of chemotactic proteins found in large quantities in PRP may be the most logical explanation. It may also be an effect of the change in scaffold mechanical properties; scaffolds with higher PRGF content exhibited decreased mechanical properties that may have allowed for cellular migration into the scaffold to occur more readily. The presence of PRGF fibers intermingled among the polymer fibers of the scaffolds, particularly in the case of the PCL:PRGF(2-1) and PCL:PRGF structures (Fig. 3), may have also provided paths of easy entry into the thicknesses of the structures. These fibers of varying diameter had an apparent impact on

**FIG. 10.** Results of macrophage proliferation when cultured on PRGF-containing scaffolds. \*Statistically significant differences between material groups of the same day,  $p < 0.05$ . TCPS, tissue culture polystyrene.



the porosity of the scaffolds. As PRGF content increased, there was an increase in fiber diameter/pore area, which may have allowed for more rapid cellular infiltration while decreasing mechanical properties.

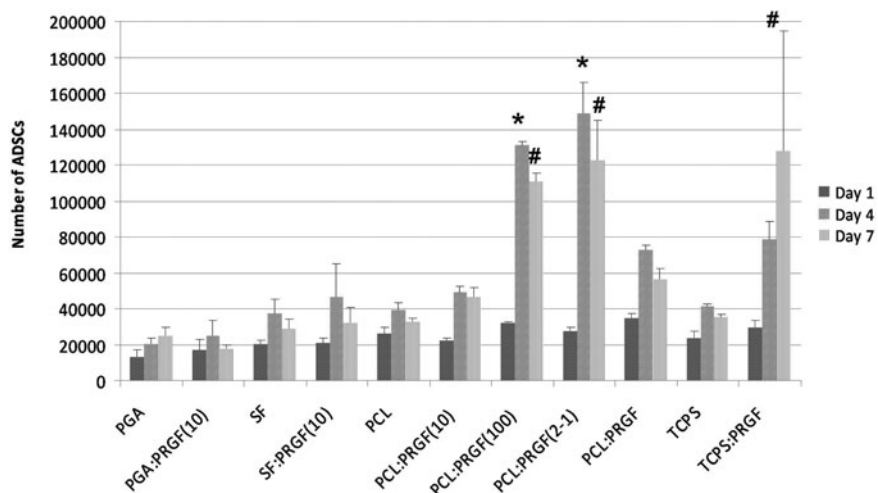
While the significant decrease in scaffold mechanical properties observed with the addition of large quantities of PRGF makes these scaffolds less than ideal for use in load-bearing tissue engineering applications, it was not completely surprising to the authors, nor was it seen as a negative result. As previously mentioned, this decrease in individual fiber mechanical properties may have contributed to the rapid cellular infiltration of the scaffolds. This enhanced cellular infiltration, regardless of its root cause, would allow for a tissue-engineered product to be more rapidly remodeled with native collagen extracellular matrix, the production of which would readily supplement the strength of the scaffolds and encourage incorporation into surrounding tissues. Although not investigated in this study, the many factors found in PRGF have been proven to increase collagen matrix production in a number of cell types.<sup>2,3,39,49</sup> TGF- $\beta$ , one such well-known matrix production-related growth factor, was released by the electrospun scaffolds in detectable quantities, in some cases for up to 21 days. Should the presence of TGF- $\beta$  and the other matrix production enhancing growth factors be actively taken up by the cells, it would be possible for accelerated matrix production to occur, and could therefore

improve the mechanical strength of the weakened PRGF-containing scaffolds.

With the creation of individual PRGF fibers within the electrospun scaffolds containing high concentrations of PRGF (SF:PRGF(100), PGA:PRGF(100), PCL:PRGF(100), PCL:PRGF(2-1), and PCL:PRGF), the loss of mechanical strength was not surprising. These PRGF fibers, consisting of a fibrinogen backbone mixed with any number of blood- and platelet-based proteins, lack inherent mechanical strength.<sup>22</sup> Similar in composition to electrospun fibrinogen,<sup>27,29</sup> which performs best mechanically when blended with synthetic polymers, and the presence of which can significantly decrease scaffold mechanical strength, the PRGF fibers are best utilized in a role of enhancing scaffold bioactivity rather than load bearing.

As demonstrated in the protein release assays conducted herein, detectable levels of proteins were released from the electrospun scaffolds for up to 35 days *in vitro*. While it can be assumed that a large percentage of the released proteins were in fact albumin and other blood proteins, not growth factors, the fact that RANTES, PDGF-BB, and TGF- $\beta$  were detectable in specific materials at up to 21 days attests to the sustained release nature of the structures. RANTES, PDGF-BB, and TGF- $\beta$  release were analyzed as they are three of the more highly concentrated proteins contained within PRP/PRGF<sup>1</sup>; however, from these results it can be interpolated

**FIG. 11.** Results of ADSC MTS assay when cultured with macrophage-conditioned medium. \*Statistically significant differences,  $p < 0.05$ , between material groups at day 4. #Statistically significant differences,  $p < 0.05$ , between material groups at day 7. ADSC, adipose-derived stem cell.



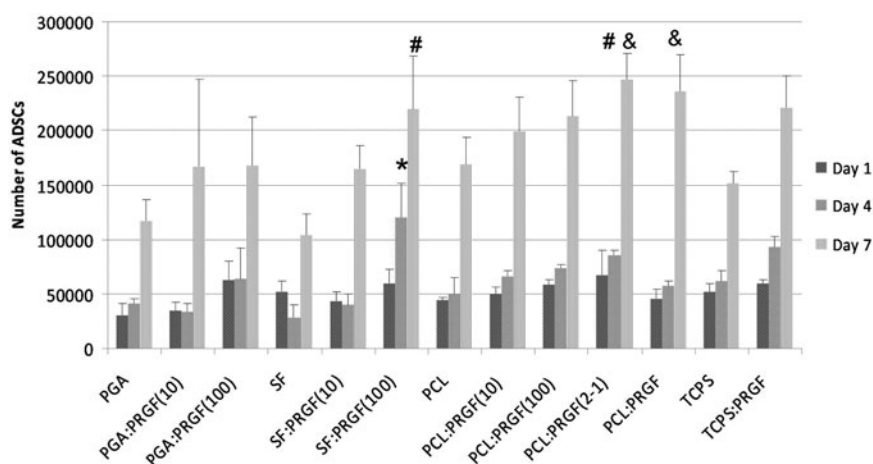


**FIG. 12.** Results of ADSC MTS assay when cultured without macrophage-conditioned medium. \*Statistically significant differences,  $p < 0.05$ , between PRGF-containing scaffolds and their control scaffolds at day 4. #Statistically significant differences,  $p < 0.05$ , between PRGF-containing scaffolds and their control scaffolds at day 7. &Statistically significant differences,  $p < 0.05$ , between PRGF-containing scaffolds and the TCPS control at day 7.

that other factors such as PDGF-AB, FGF, and EGF will be released in the same fashion. The nature of the release demonstrated from the electrospun scaffolds may prove to be effective in proposed *in vivo* follow-up studies at enhancing migration of cells from surrounding tissues, with a large burst of protein creating a substantial chemotactic gradient, followed by a sustained release of protein to promote cell proliferation, and scaffold infiltration and remodeling. The incorporation and subsequent release of albumin, while seemingly inconsequential, may in fact serve as a protectant for the cytokines and chemokines included in the PRGF. The hydrophilic albumin molecules have been demonstrated in the literature to have the potential to encapsulate smaller proteins, and effectively shield them from potential denaturation.<sup>50,51</sup>

The retention of PRGF's biological activity after the electrospinning process, subjected to both high voltages and the organic solvent HFP, is displayed in the ADSC response to conditioned medium from PRGF-containing scaffolds cultured with and without macrophages. In both cases, ADSC proliferation was enhanced over 7 days when cultured in conditioned medium from scaffolds containing PRGF versus those not containing PRGF. The presence of several growth factors within PRGF known to induce cell proliferation (VEGF, PDGF, IGF, FGF, and EGF, etc.) is most likely the reason for enhanced ADSC proliferation<sup>2</sup>; however, future ELISA analysis will be needed to confirm this. Their proliferation profile over the 7 days was different depending on the presence or absence of macrophages, alluding to the fact that ADSC proliferation was affected by the interaction of macrophages with PRGF-containing scaffolds. It is evident from this study that macrophage number is not the most critical factor in ADSC proliferation; however, the specific mechanism by which macrophage interaction with the scaffolds affects ADSC proliferation was not specifically explored.

The authors hypothesize that the ADSC proliferation seen in this study might be due, in part, to the various growth factors and cytokines secreted by the macrophages. It has been shown previously that macrophages cultured on electrospun scaffolds have the ability to produce high levels of VEGF and FGF<sup>52</sup> and, in the presence of PRGF, produce additional pro-angiogenic growth factors and cytokines, including those that enhance cell proliferation.<sup>1</sup> Although

ADSC proliferation appeared to stop by day 7 when cultured in macrophage-conditioned medium, this was not perceived as a negative effect brought about by the presence of PRGF, rather most likely due to medium mismatch and/or harmful factors produced during macrophage apoptosis induced by a lack of nutrient supply in the conditioned medium.<sup>38</sup>

In conclusion, this study demonstrated the potential for PRP to be subjected to an FTF process, lyophilized to create PRGF, and incorporated into electrospun scaffolds of various materials. This PRGF was released from the electrospun scaffolds in a controlled fashion over a period of 35 days in culture, and retained its potential to positively influence the proliferation of ADSCs and chemotaxis of macrophages at specific concentrations *in vitro*. Additionally, the presence of PRGF in high concentrations allowed for the rapid infiltration of ADSCs into electrospun structures of both natural and synthetic polymers when cultured *in vitro* for 21 days. Additional studies are needed to determine what effect the presence of PRGF will have *in vivo* on the recruitment of cells from the surrounding tissues, and the cellularization and remodeling of the electrospun structures. As one of the major advantages of PRP, when used clinically, is its ability to deliver a milieu of growth factors and cytokines at the patients' bedside, the creation of an off-the-shelf electrospun scaffold incorporating PRGF from pooled allogenic blood may have the same benefits. While the use of pooled blood is typically frowned upon in the United States, the use of allogenic PRP has been gaining popularity in a number of European studies with no mention of adverse immune reactions.<sup>53-56</sup>

### Acknowledgments

The authors would like to thank Drs. Sherwin Kevy and May Jacobsen from the Harvard Immune Disease Institute's Blood Research Laboratory for conducting platelet counts on pooled whole blood and PRP. The authors would also like to thank Anatomic Pathology Research Services in the Department of Pathology at Virginia Commonwealth University for histological staining. SEM was performed at the Virginia Commonwealth University Department of Anatomy and Neurobiology Microscopy Facility, supported in part with funding from NIH-NINDS Center core grant (5P30NS047463-02).

## Disclosure Statement

No competing financial interests exist.

## References

- El-Sharkawy, H., Kantarci, A., Deady, J., Hasturk, H., Liu, H., Alshahat, M., and Van Dyke, T.E. Platelet-rich plasma: growth factors and pro- and anti-inflammatory properties. *J Periodontol* **78**, 661, 2007.
- Foster, T.E., Puskas, B.L., Mandelbaum, B.R., Gerhardt, M.B., and Rodeo, S.A. Platelet-rich plasma: from basic science to clinical applications. *Am J Sports Med* **37**, 2259, 2009.
- Rozman, P., and Bolta, Z. Use of platelet growth factors in treating wounds and soft-tissue injuries. *Acta Dermatovenol Alp Panonica Adriat* **16**, 156, 2007.
- Everts, P.A., Knape, J.T., Weibrich, G., Schonberger, J.P., Hoffmann, J., Overvest, E.P., Box, H.A., and van Zundert, A. Platelet-rich plasma and platelet gel: a review. *J Extra Corpor Technol* **38**, 174, 2006.
- Sanchez, M., Anitua, E., Orive, G., Mujika, I., and Andia, I. Platelet-rich therapies in the treatment of orthopaedic sport injuries. *Sports Med* **39**, 345, 2009.
- Creaney, L., and Hamilton, B. Growth factor delivery methods in the management of sports injuries: the state of play. *Br J Sports Med* **42**, 314, 2008.
- Alsousou, J., Thompson, M., Hulley, P., Noble, A., and Willett, K. The biology of platelet-rich plasma and its application in trauma and orthopaedic surgery: a review of the literature. *J Bone Joint Surg Br* **91**, 987, 2009.
- Anitua, E., Sanchez, M., Orive, G., and Andia, I. Delivering growth factors for therapeutics. *Trends Pharmacol Sci* **29**, 37, 2008.
- Lyras, D.N., Kazakos, K., Verettas, D., Botaitis, S., Agrogiannis, G., Kokka, A., Pitiakoudis, M., and Kotzakis, A. The effect of platelet-rich plasma gel in the early phase of patellar tendon healing. *Arch Orthop Trauma Surg* **129**, 1577, 2009.
- Murray, M.M., Spindler, K.P., Abreu, E., Muller, J.A., Nelder, A., Kelly, M., Frino, J., Zurakowski, D., Valenza, M., Snyder, B.D., *et al.* Collagen-platelet rich plasma hydrogel enhances primary repair of the porcine anterior cruciate ligament. *J Orthop Res* **25**, 81, 2007.
- Mishra, A., and Pavelko, T. Treatment of chronic elbow tendinosis with buffered platelet-rich plasma. *Am J Sports Med* **34**, 1774, 2006.
- Anitua, E., Aguirre, J.J., Algorta, J., Ayerdi, E., Cabezas, A.I., Orive, G., and Andia, I. Effectiveness of autologous preparation rich in growth factors for the treatment of chronic cutaneous ulcers. *J Biomed Mater Res B Appl Biomater* **84**, 415, 2008.
- Kocaoemer, A., Kern, S., Kluter, H., and Bieback, K. Human AB serum and thrombin-activated platelet-rich plasma are suitable alternatives to fetal calf serum for the expansion of mesenchymal stem cells from adipose tissue. *Stem Cells* **25**, 1270, 2007.
- Lu, H.H., Vo, J.M., Chin, H.S., Lin, J., Cozin, M., Tsay, R., Eisig, S., and Landesberg, R. Controlled delivery of platelet-rich plasma-derived growth factors for bone formation. *J Biomed Mater Res A* **86**, 1128, 2008.
- Bir, S.C., Esaki, J., Marui, A., Yamahara, K., Tsubota, H., Ikeda, T., and Sakata, R. Angiogenic properties of sustained release platelet-rich plasma: characterization *in-vitro* and in the ischemic hind limb of the mouse. *J Vasc Surg* **50**, 870 e2, 2009.
- Pietramaggiore, G., Kaipainen, A., Czezug, J.M., Wagner, C.T., and Orgill, D.P. Freeze-dried platelet-rich plasma shows beneficial healing properties in chronic wounds. *Wound Repair Regen* **14**, 573, 2006.
- Pietramaggiore, G., Kaipainen, A., Ho, D., Orser, C., Pebley, W., Rudolph, A., and Orgill, D.P. Trehalose lyophilized platelets for wound healing. *Wound Repair Regen* **15**, 213, 2007.
- Pietramaggiore, G., Scherer, S.S., Mathews, J.C., Alperovich, M., Yang, H.J., Neuwalder, J., Czezug, J.M., Chan, R.K., Wagner, C.T., and Orgill, D.P. Healing modulation induced by freeze-dried platelet-rich plasma and micronized allogenic dermis in a diabetic wound model. *Wound Repair Regen* **16**, 218, 2008.
- Sum, R., Hager, S., Pietramaggiore, G., Orgill, D.P., Dee, J., Rudolph, A., Orser, C., Fitzpatrick, G.M., and Ho, D. Wound-healing properties of trehalose-stabilized freeze-dried outdated platelets. *Transfusion* **47**, 672, 2007.
- Sell, S.A., McClure, M.J., Ayres, C.E., Simpson, D.G., and Bowlin, G.L. Preliminary investigation of airgap electrospun silk fibroin-based structures for ligament analogue engineering. *J Biomater Sci Polym Ed* **22**, 1253, 2011.
- Altman, G.H., Horan, R.L., Lu, H.H., Moreau, J., Martin, I., Richmond, J.C., and Kaplan, D.L. Silk matrix for tissue engineered anterior cruciate ligaments. *Biomaterials* **23**, 4131, 2002.
- Wolfe, P.S., Sell, S.A., Ericksen, J.J., Simpson, D.G., and Bowlin, G.L. The creation of electrospun nanofibers from platelet-rich plasma. *J Tissue Sci Eng* 2011 [Epub ahead of print]; DOI: 10.4172/2157-7552.1000107.
- Kevy, S.V., and Jacobson, M.S. Comparison of methods for point of care preparation of autologous platelet gel. *J Extra Corpor Technol* **36**, 28, 2004.
- Jacobson, M., Fufa, D., Abreu, E.L., Kevy, S., and Murray, M.M. Platelets, but not erythrocytes, significantly affect cytokine release and scaffold contraction in a provisional scaffold model. *Wound Repair Regen* **16**, 370, 2008.
- Boland, E.D., Coleman, B.D., Barnes, C.P., Simpson, D.G., Wnek, G.E., and Bowlin, G.L. Electrospinning polydioxanone for biomedical applications. *Acta Biomaterialia* **1**, 115, 2005.
- Boland, E.D., Wnek, G.E., Simpson, D.G., Pawlowski, K.J., and Bowlin, G.L. Tailoring tissue engineering scaffolds using electrostatic processing techniques: A study of poly(glycolic acid) electrospinning. *J Macromol Sci A38*, 1231, 2001.
- McManus, M.C., Boland, E.D., Koo, H.P., Barnes, C.P., Pawlowski, K.J., Wnek, G.E., Simpson, D.G., and Bowlin, G.L. Mechanical properties of electrospun fibrinogen structures. *Acta Biomater* **2**, 19, 2006.
- Barnes, C.P., Sell, S.A., Knapp, D.C., Walpoth, B.H., Brand, D.D., and Bowlin, G.L. Preliminary investigation of electrospun collagen and polydioxanone for vascular tissue engineering applications. *Int J Electrospun Nanofiber Appl* **1**, 73, 2007.
- McManus, M.C., Sell, S.A., Bowen, W.C., Koo, H.P., Simpson, D.G., and Bowlin, G.L. Electrospun fibrinogen-polydioxanone composite matrix: Potential for *in situ* urologic tissue engineering. *J Eng Fiber Fabric* **3**, 12, 2008.
- Sell, S.A., McClure, M.J., Barnes, C.P., Knapp, D.C., Walpoth, B.H., and Simpson, D.G., Bowlin, G.L. Electrospun polydioxanone-elastin blends: potential for bioresorbable vascular grafts. *Biomed Mater* **1**, 72, 2006.
- Baker, B.M., Gee, A.O., Metter, R.B., Nathan, A.S., Marklein, R.A., Burdick, J.A., and Mauck, R.L. The potential to improve cell infiltration in composite fiber-aligned electrospun scaffolds by the selective removal of sacrificial fibers. *Biomaterials* **29**, 2348, 2008.

32. Baker, B.M., Nerurkar, N.L., Burdick, J.A., Elliott, D.M., and Mauck, R.L. Fabrication and modeling of dynamic multipolymer nanofibrous scaffolds. *J Biomech Eng* **131**, 101012, 2009.
33. Lucarelli, E., Beccheroni, A., Donati, D., Sangiorgi, L., Cencacchi, A., Del Vento, A.M., Meotti, C., Bertoja, A.Z., Giardino, R., Fornasari, P.M., *et al.* Platelet-derived growth factors enhance proliferation of human stromal stem cells. *Biomaterials* **24**, 3095, 2003.
34. Mishra, A., Tummala, P., King, A., Lee, B., Kraus, M., Tse, V., and Jacobs, C.R. Buffered platelet-rich plasma enhances mesenchymal stem cell proliferation and chondrogenic differentiation. *Tissue Eng Part C Methods* **15**, 431, 2009.
35. Vogel, J.P., Szalay, K., Geiger, F., Kramer, M., Richter, W., and Kasten, P. Platelet-rich plasma improves expansion of human mesenchymal stem cells and retains differentiation capacity and *in vivo* bone formation in calcium phosphate ceramics. *Platelets* **17**, 462, 2006.
36. Anitua, E., Sanchez, M., Zalduendo, M.M., de la Fuente, M., Prado, R., Orive, G., and Andia, I. Fibroblastic response to treatment with different preparations rich in growth factors. *Cell Prolif* **42**, 162, 2009.
37. Kakudo, N., Minakata, T., Mitsui, T., Kushida, S., Notodihardjo, F.Z., and Kusumoto, K. Proliferation-promoting effect of platelet-rich plasma on human adipose-derived stem cells and human dermal fibroblasts. *Plast Reconstr Surg* **122**, 1352, 2008.
38. Seimon, T., and Tabas, I. Mechanisms and consequences of macrophage apoptosis in atherosclerosis. *J Lipid Res* **50 Suppl**, S382, 2009.
39. Cheng, M., Wang, H., Yoshida, R., and Murray, M.M. Platelets and plasma proteins are both required to stimulate collagen gene expression by anterior cruciate ligament cells in three-dimensional culture. *Tissue Eng Part A* **16**, 1479, 2010.
40. Gassling, V.L., Acil, Y., Springer, I.N., Hubert, N., and Wiltfang, J. Platelet-rich plasma and platelet-rich fibrin in human cell culture. *Oral Surg Oral Med Oral Pathol Oral Radiol Endod* **108**, 48, 2009.
41. Lei, H., Xiao, R., Tang, X.J., and Gui, L. Evaluation of the efficacy of platelet-rich plasma in delivering BMSCs into 3D porous scaffolds. *J Biomed Mater Res B Appl Biomater* **91**, 679, 2009.
42. Sahoo, S., Ang, L.T., Goh, J.C., and Toh, S.L. Growth factor delivery through electrospun nanofibers in scaffolds for tissue engineering applications. *J Biomed Mater Res A* **93**, 1539, 2010.
43. Sahoo, S., Toh, S.L., and Goh, J.C. A bFGF-releasing silk/PLGA-based biohybrid scaffold for ligament/tendon tissue engineering using mesenchymal progenitor cells. *Biomaterials* **31**, 2990, 2010.
44. Uebersax, L., Merkle, H.P., and Meinel, L. Biopolymer-based growth factor delivery for tissue repair: from natural concepts to engineered systems. *Tissue Eng Part B Rev* **15**, 263, 2009.
45. Chew, S.Y., Wen, J., Yim, E.K., and Leong, K.W. Sustained release of proteins from electrospun biodegradable fibers. *Biomacromolecules* **6**, 2017, 2005.
46. Zhang, G., and Suggs, L.J. Matrices and scaffolds for drug delivery in vascular tissue engineering. *Adv Drug Deliv Rev* **59**, 360, 2007.
47. Chung, H.J., and Park, T.G. Surface engineered and drug releasing pre-fabricated scaffolds for tissue engineering. *Adv Drug Deliv Rev* **59**, 249, 2007.
48. Chen, F.M., Zhang, M., and Wu, Z.F. Toward delivery of multiple growth factors in tissue engineering. *Biomaterials* **31**, 6279, 2010.
49. Visser, L.C., Arnoczky, S.P., Caballero, O., Kern, A., Ratcliffe, A., and Gardner, K.L. Growth factor-rich plasma increases tendon cell proliferation and matrix synthesis on a synthetic scaffold: an *in vitro* study. *Tissue Eng Part A* **16**, 1021, 2010.
50. Johnson, P.J., Skornia, S.L., Stabenfeldt, S.E., and Willits, R.K. Maintaining bioactivity of NGF for controlled release from PLGA using PEG. *J Biomed Mater Res A* **86**, 420, 2008.
51. Nimni, M.E. Polypeptide growth factors: targeted delivery systems. *Biomaterials* **18**, 1201, 1997.
52. Garg, K., Sell, S.A., Madurantakam, P., and Bowlin, G.L. Angiogenic potential of human macrophages on electrospun bioresorbable vascular grafts. *Biomed Mater* **4**, 031001, 2009.
53. Scevola, S., Nicoletti, G., Brenta, F., Isernia, P., Maestri, M., and Faga, A. Allogenic platelet gel in the treatment of pressure sores: a pilot study. *Int Wound J* **7**, 184, 2010.
54. Bernuzzi, G., Tardito, S., Bussolati, O., Adorni, D., Cantarelli, S., Fagnoni, F., Rossetti, A., Azzarone, M., Ficarelli, E., Caleffi, E., *et al.* Platelet gel in the treatment of cutaneous ulcers: the experience of the Immunohaematology and Transfusion Centre of Parma. *Blood Transfus* **8**, 237, 2010.
55. Senet, P., Bon, F.X., Benbunan, M., Bussel, A., Traineau, R., Calvo, F., Dubertret, L., and Dosquet, C. Randomized trial and local biological effect of autologous platelets used as adjuvant therapy for chronic venous leg ulcers. *J Vasc Surg* **38**, 1342, 2003.
56. Chen, T.M., Tsai, J.C., and Burnouf, T. A novel technique combining platelet gel, skin graft, and fibrin glue for healing recalcitrant lower extremity ulcers. *Dermatol Surg* **36**, 453, 2010.

Address correspondence to:

Scott A. Sell, Ph.D.

Physical Medicine and Rehabilitation  
Hunter Holmes McGuire VA Medical Center  
1201 Broad Rock Blvd.  
Richmond, VA 23249

E-mail: s2sasell@vcu.edu

Received: November 15, 2010

Accepted: June 15, 2011

Online Publication Date: September 5, 2011

